J. of Basic Sciences, Cheju Nat'l Univ.
15(1), 7~13, 2002

기초과학연구 제주대학교
15(1), 7~13, 2002

Refractive Elastic Scattering of $^{16}O + ^{16}O$ System at $E_{lab} = 250$ MeV

Yong Joo Kim and Nam Gyu Hyun
Department of Physics and Research Institute for Basic Sciences, Cheju National University, Jeju 690-756
Dong Shik Kang
Department of Science Education, Cheju National University, Jeju 690-756

The experimental data on elastic $^{16}O + ^{16}O$ scattering at $E_{lab} = 250$ MeV has been analyzed within the first-order eikonal model based on Coulomb trajectories of colliding nuclei. The presence of nuclear rainbow in this system is evidenced through a classical deflection function. We have found that the strong real and weak imaginary optical potentials are required to describe the refractive $^{16}O + ^{16}O$ elastic scatterings at $E_{lab} = 250$ MeV. The refractive pattern could be shown to be sensitive to the real part of optical potential at small radius.

I. INTRODUCTION

Study of light heavy-ion elastic scattering at intermediate energies has received considerable attention in recent years. Usually the heavy-ion elastic scattering is dominated by the strong absorption, which the implication that the data are only sensitive to the surface of the interaction region. Therefore, the optical potential required to describe the measurements is not uniquely determined. However, the angular distribution for light heavy-ion elastic scattering such as $^{12}C + ^{12}C$ and $^{16}O + ^{16}O$ systems has shown the presence of strong refractive effects. The refractive (rainbow) phenomena in nuclear elastic scattering provide a unique source of information on the heavy-ion interaction potential at small internuclear distance.

Over the past years there are several efforts [1-8] to describe the refractive scattering pattern between the light heavy-ions. Bartnitzky *et al.* [4] have measured the elastic scattering cross section for ^{16}O ions on ^{16}O targets with high accuracy over large angular ranges at incident energies from 250 to 704 MeV, and extracted the underlying scattering potentials using model-unrestricted analysis. The experimental data on elastic $^{16}O + ^{16}O$ scattering at incident energies ranging from 124 to 1120 MeV have been analyzed [7] within the standard optical model, using either the phenomenological potential (Wood-Saxon squared) or that calculated within the double-folding model for real part of the optical potential. Brandan *et al.* [8] have measured the $^{16}O + ^{12}C$ elastic cross section at 300 MeV over a wide angular range, displaying the shoulder of a nuclear rainbow, and analyzed this data using the optical model.

By the way, a number of studies [9-11] have been made to describe the elastic scattering processes between heavy ions within the framework of the eikonal model [12,13]. Aguiar *et al.* [11] have discussed different schemes devised to extend the eikonal approximation to the regime of low bombarding energies in heavy-ion collisions. In our previous paper [14], we have presented the first- and second-order corrections to the zeroth-order eikonal phase shifts for heavy-ion elastic scatterings based on Coulomb trajectories of colliding nuclei and it has been applied satisfactorily to the $^{16}O + ^{40}Ca$ and $^{16}O + ^{90}Zr$ systems at $E_{lab} = 1503$ MeV. The elastic scatterings of $^{12}C + ^{12}C$ system at $E_{lab} = 240$, 360 and 1016 MeV are analyzed using the first-order non-eikonal correction to the eikonal phase shift [15].

The measurements of elastic angular distributions for the ^{16}O ions on ^{16}O at intermediate energies have attracted considerable

interest, since they show a strongly refractive pattern in the angular distribution. Almost all studies [2,4,7] of $^{16}O + ^{16}O$ elastic scattering have been made within the optical model or folding model. In this work, we analyze the elastic scattering angular distributions of the $^{16}O + ^{16}O$ system at E_{lab}=250 MeV by using the first-order eikonal model. The presence of nuclear rainbow is examined. We also investigate some features of the effective optical potential and phase shift. In section II, we present the theory related with first-order eikonal model. Section III contains the results and discussions. Finally, section IV concludes the paper.

II. THEORY

The Coulomb-modified eikonal phase shift and its first-order correction are given by [14]

$$\delta_L^0(r_c) = -\frac{\mu}{\hbar^2 k}\int_0^\infty U(r)\,dz, \quad (1)$$

$$\delta_L^1(r_c) = -\frac{\mu^2}{2\hbar^4 k^3}\left(1 + r_c\frac{d}{dr_c}\right)\int_0^\infty U^2(r)\,dz, \quad (2)$$

where $r = \sqrt{r_c^2 + z^2}$, μ is the reduced mass and the distance of closet approach r_c is given by

$$r_c = \frac{1}{k}\left\{\eta + \left[\eta^2 + (L+\frac{1}{2})^2\right]^{1/2}\right\}, \quad (3)$$

with the Sommerfeld parameter η.

The zeroth-order term in this expansion is the ordinary eikonal approximation phase shift function, while the corrections given by first-order term correspond to non-eikonal effects. The first-order eikonal correction term of the phase shift, $\delta_L^1(r_c)$ in Eqs. (2), can further be expressed as following

$$\delta_L^1(r_c) = -\frac{\mu^2}{\hbar^4 k^3}\int_0^\infty \left[U^2(r) + rU(r)\frac{dU(r)}{dr}\right] dz. \quad (4)$$

The closed expression of the effective phase shift function including up to the first-order correction term may be written as

$$\delta_L(r_c) = -\frac{\mu}{\hbar^2 k}\int_0^\infty U_{\rm eff}(r)\,dz, \quad (5)$$

where $U_{\rm eff}(r)$ is the effective optical potential given by

$$U_{\rm eff}(r) = U\left\{1 + \frac{\mu}{\hbar^2 k^2}\left[U + r\frac{dU}{dr}\right]\right\}. \quad (6)$$

We can see that the phase shift calculation including non-eikonal corrections up to the first-order is equivalent to a zeroth-order calculation with effective potential $U_{\rm eff}(r)$. By taking $U(r)$ as the optical Woods-Saxon forms given by

$$U(r) = -\frac{V_0}{1+e^{(r-R_v)/a_v}} - i\frac{W_0}{1+e^{(r-R_w)/a_w}}, \quad (7)$$

with $R_{v,w} = r_{v,w}(A_1^{1/3} + A_2^{1/3})$, we can use the effective phase shift, Eq.(5) in the general expression for the elastic scattering cross section.

The general expression of the differential cross section between two identical spinless nuclei is given by the following formula

$$\frac{d\sigma}{d\Omega} = |f(\theta) + f(\pi-\theta)|^2, \quad (8)$$

where elastic scattering amplitude $f(\theta)$ is given by the equation

$$f(\theta) = f_{\rm R}(\theta) + \frac{1}{ik}\sum_{L=0}^{\infty}(L+\frac{1}{2})\exp(2i\sigma_L)(S_L^{\rm N}-1)P_L(\cos\theta). \quad (9)$$

Here $f_{\rm R}(\theta)$ is the usual Rutherford scattering amplitude, k is the wave number and σ_L the Coulomb phase shifts. The nuclear S-matrix elements S_L^N can be expressed by the nuclear phase shifts δ_L

$$S_L^N = \exp(2i\delta_L). \quad (10)$$

Since the nuclear phase shifts are complex, the variations of the Coulomb and real parts of the nuclear phase shifts over L give the deflection function

$$\theta_L = 2\frac{d}{dL}(\sigma_L + \text{Re }\delta_L). \quad (11)$$

This deflection angle is a semiclassical treatment of a trajectory with orbital angular momentum L.

TABLE I: Parameters of the fitted Woods-Saxon potential by using the first-order eikonal model analysis for the ^{16}O + ^{16}O elastic scattering at E_{lab}= 250 MeV. 10 % error bars are adopted to obtain χ^2/N value.

V_0 (MeV)	r_v (fm)	a_v (fm)	W_0 (MeV)	r_w (fm)	a_w (fm)	σ_R (mb)	χ^2/N δ^0	$\delta^0+\delta^1$
223	0.815	0.753	42.9	1.062	0.732	1757	56.45	7.68

TABLE II: Parameters of best fitted Woods-Saxon potential by using the eikonal approximation analysis for ^{16}O + ^{16}O elastic scattering at E_{lab}= 250 MeV. 10 % error bars are adopted to obtain χ^2/N value.

V_0 (MeV)	r_v (fm)	a_v (fm)	W_0 (MeV)	r_w (fm)	a_w (fm)	σ_R (mb)	χ^2/N
242	0.835	0.729	39.5	1.137	0.658	1731	10.24

III. RESULTS AND DISCUSSIONS

The elastic differential cross section for ^{16}O + ^{16}O systems at E_{lab}= 250 MeV is calculated by using the first-order Coulomb-modified eikonal model. The Woods-Saxon potential parameters obtained from first-order eikonal model and eikonal approximation fits to the experimental data are listed in Table I and II. The calculated results of the differential cross sections for the elastic scattering of ^{16}O + ^{16}O systems at E_{lab}= 250 MeV are presented in Fig. 1 together with the observed data [4]. In this figure, the dotted and solid curve are the results for the zeroth-order eikonal phase shift and its first-order corrections, respectively. As seen in this figure, there are the substantial differences between the dotted and solid curves when compared to the experimental data. Two calculated angular distributions are nearly identical at forward angles but are qualitatively different at large angles. The present result of first-order eikonal model can reproduce satisfactorily the observed data over the whole angular range. The reasonable χ^2/N value is obtained in the ^{16}O + ^{16}O system at E_{lab}= 250 MeV as listed in Table I. In order to investigate the first-order eikonal correction to the zeroth-order eikonal phase shift, the best calculated cross section using the common eikonal approximation is presented in Fig.1 as a dashed curve. The best fitted Woods-Saxon potential parameters by the eikonal approximation are listed in Table II. The result by

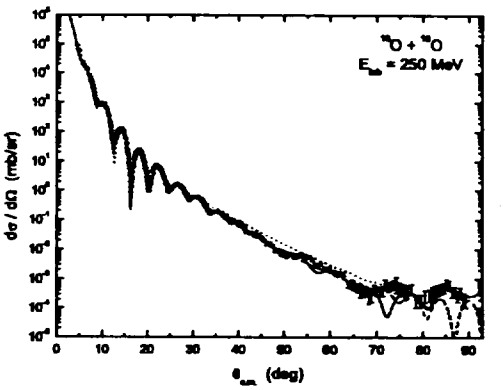

FIG. 1: Elastic scattering angular distributions for ^{16}O + ^{16}O system at E_{lab}= 250 MeV. The solid circles denote the observed data taken from Ref.[4]. The solid and dotted curves are the results for first- and zeroth-order eikonal corrections, respectively. The dashed curve is the best result from the eikonal approximation using the potential parameters given in Table 2.

the using first-order eikonal model provides more reasonable fit to the refractive structure at large angles compared with one by using eikonal approximation. We can see in Tables I and II that the value of χ^2/N decreases in the calculated result with the first-order eikonal model compared to the one with eikonal approximation.

The transparency function $T_L = |S_L|^2$ is

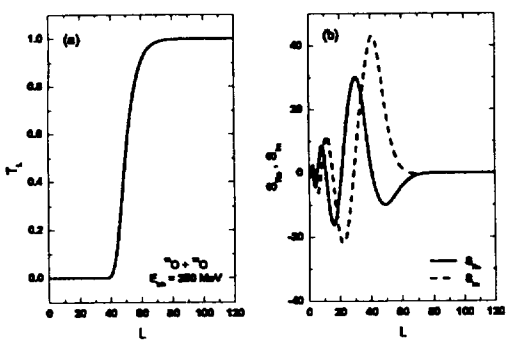

FIG. 2: (a) Transparency function and (b) the real and imaginary parts of the term $i(L+\frac{1}{2})\exp(2i\sigma_L)(S_L^N-1)$ for the $^{16}O+^{16}O$ system at E_{lab}= 250 MeV plotted versus the orbital angular momentum L in the first-order eikonal model

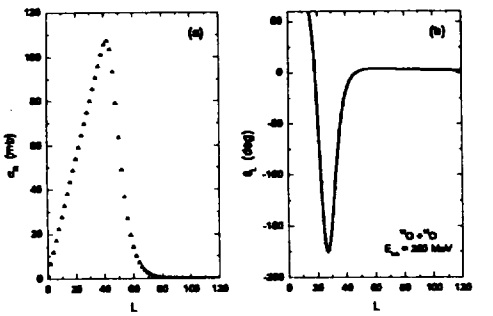

FIG. 3: (a) Partial wave reaction cross section and (b) deflection function for ^{16}O + ^{16}O system at E_{lab}= 250 MeV plotted versus the orbital angular momentum L in the first-order eikonal model.

plotted versus the orbital angular momentum in Fig.2, along with the real and imaginary parts of the term $i(L+\frac{1}{2})\exp(2i\sigma_L)(S_L^N-1)$ for the ^{16}O + ^{16}O system at E_{lab}= 250 MeV. The transparency function can be explained using the imaginary part of the effective optical potential. As shown Fig. 2(a), the lower partial waves are totally absorbed and the T_L is increased very rapidly in a narrow localized angular momenta zone. The term $i(L+\frac{1}{2})\exp(2i\sigma_L)(S_L^N-1)$ represents the partial wave contributions to the cross section in terms of angular momentum. We can see that partial waves larger than L = 90 do not nearly contribute the elastic cross section of this system.

In figure 3, we plot the partial wave reaction cross section and deflection function as a function of angular momentum for ^{16}O + ^{16}O system at E_{lab}= 250 MeV. We found in Fig.3(a) that the value of the partial reaction cross section increases linearly up to L = 42. Beyond this L value, the partial reaction cross section decreases quadratically. When the absorptive potential is weak and the real potential is strong, it is known that the contribution to the scattering from the interior region is large enough to be observed. By analogy to optics, these contributions are called refractive, since the scattered particles have partially penetrated the target nucleus. This situation is interpreted as a "nuclear rainbow scattering", because the intensity maximum is built by many trajectories being essentially deflected through the same scattering angle; The nuclear rainbow angle is obtained from the classical deflection function given by Eq.(11). In a rainbow situation, the strong nuclear force attracts the projectiles towards the scattering center and deflects them to negative angle, which correspond to the region of the rainbow maximum. In Fig. 3(b), we can find the nuclear rainbow angle value $\theta_{nr} = -176.0^o$ at L = 27, which evidently proves a presence of the nuclear rainbow with unambiguous clarity in this system.

In figure 4, we plot the real and imaginary parts of effective potential in Eq.(6) and nominal potential in Eq.(7), and examine the effect of first-order non-eikonal correction. The solid curve is the first-order effective potentials $U_{\rm eff}(r)$ given by Eq.(6), while the dashed curve is the result of nominal potential $U(r)$ given by Eq.(7). As shown in these figures, there is a dramatic difference between two potentials, especially for the imaginary part. We can see in Eq.(6) that the effective imaginary potential with the first-order eikonal correction depends on the product of the real and imaginary potentials and their derivatives. Thus the effective imaginary poten-

tial rapidly increases until it reaches maximum value in the central region of the nucleus, and then it reaches minimum near the surface region. A drastic increase of the imaginary potential for small values of r is mainly due to the correction term in Eq.(6). The imaginary part of potential itself provides the radial weighting of flux removal from the entrance channel, and is consequently responsible for the absorption process in the nuclear reaction. In the ordinary eikonal model, the shape of imaginary potential should not be affected by the real potential. Nevertheless, in the present eikonal model with the first-order correction, we can find that the drastic increases on the absorptive potential in the small r region are due to the larger real potential compared with imaginary one. In the small r region, the effective imaginary potential of the first-order eikonal model is small compared with the effective real potential. This implies deep, elastic interpenetration of the target and projectile, and a feature unambiguously required by the appearance of refractive phenomena in the angular distribution. These strongly real and weakly imaginary potential values lead to observe the contributions to the scattering from the interior region and allow refracted projectiles to populate the elastic channel and typical refractive phenomena could be observed in the angular distribution.

Such a increase of the effective potentials in the small r region is also reflected in the phase shift function. Figure 5 show angular momentum dependence of the real and imaginary parts of the eikonal phase shifts, respectively. The dashed and solid curves are the results for the zeroth and first-order non-eikonal corrections, respectively. The phase shift obtained without the real potential decreases monotonically with the increasing angular momentum L. However, effective phase shifts displays the different structure. Particularly, the real potential gives a drastic variations of the imaginary phase shift for ^{16}O + ^{16}O system at E_{lab}= 250 MeV. We can see in the phase shifts calculated with the real potential that an absorption of partial waves for the large angular momentum increases, whereas the absorption decrease for small angular momentum, compared with the

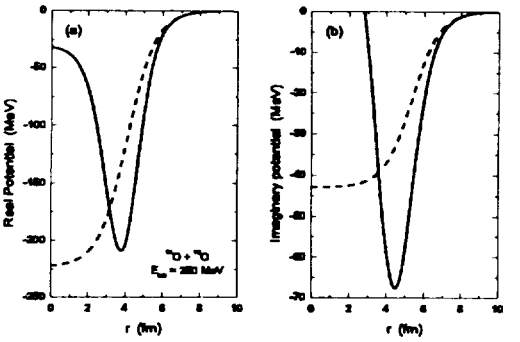

FIG. 4: (a) Real and (b) imaginary parts of the optical potential for the ^{16}O + ^{16}O system at E_{lab}= 250 MeV. The solid and dashed curves are the results for first- and zeroth-order eikonal corrections, respectively.

result without the real potential. The large angle behavior is sensitive to the details of the real optical potential over a wide radial region from the nuclear surface towards the interior. This confirms the predictions and the treatment based on the effective potential given by Eq. (6).

IV. CONCLUSIONS

In this work, the elastic scattering of ^{16}O+ ^{16}O system at E_{lab}=250 MeV has been analyzed by using the first-order eikonal model based on the Coulomb trajectories of colliding nuclei. We have found that the result of the present first-order eikonal model is in reasonable agreement with the observed data. Through the classical deflection function, we can find the nuclear rainbow angle value $\theta_{nr} = -176.0^{o}$ at $L = 27$, which evidently proves a presence of the nuclear rainbow with unambiguous clarity in this system. The strong real and and weak imaginary potentials are found and they support the presence of a nuclear rainbow in the angular distribution of this system.

We have found that the effect of first-order eikonal correction on the imaginary potential is important when the absorptive potential is weak and the real potential is strong. A

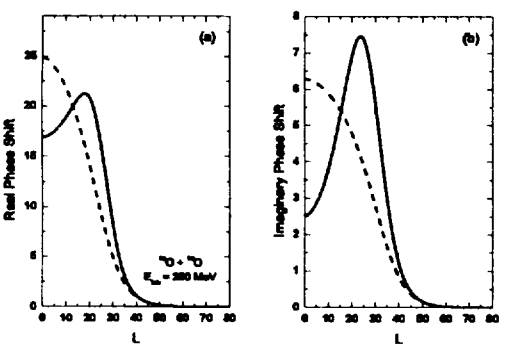

FIG. 5: (a) Real and (b) imaginary parts of the eikonal phase shift for the $^{16}O + ^{16}O$ system at E_{lab}= 250 MeV. The solid and dashed curves are the results for first- and zeroth-order eikonal corrections, respectively.

drastic increase of the imaginary potential for small values of r is mainly due to the correction term in the effective potential formula, and it is related with the larger real potential compared with imaginary one. The ratio of imaginary to real part of effective potential is found to be small in the central region. This implies deep, elastic interpenetration of the target and projectile, and a feature unambiguously required by the appearance of refractive phenomena in the angular distribution. These strongly real and weakly imaginary potential values lead to observe the contributions to the scattering from the interior region and allow refracted projectiles to populate the elastic channel and typical refractive phenomena could be observed in the angular distribution. We can also see in the imaginary phase shift calculated with the real potential that an absorption of partial waves for large angular momentum increases, whereas the absorption decreases for small angular momentum, compared to the result without the real potential. Such a behavior explains why our calculation is sensitive to the real potential at very small radius.

REFERENCES

[1] M. E. Brandan, Phys. Rev. Lett. **60**, 784 (1988).

[2] E. Stiliaris, H. G. Bohlen, P. Fröbrich, B. Gebauer, D. Kolbert, W. von Oertzen, M. Wilpert and Th. Wilpert, Phys. Lett. **223**, 291 (1989).

[3] D. T. Khoa, W.von Oertzen, H. G. Bohlen, G. Bartnitzky, H. Clement, Y. Sugiyama, B. Gebauer, A. N. Ostrowski, Th. Wilpert and C. Langner, Phys. Rev. Lett. **74**, 34 (1995).

[4] G. Bartnitzky, A. Blazevic, H. G. Bohlen, J. M. Casandjian, M. Chartier, H. Clement, B. Gebauer, A. Gillibert, Th. Kirchner, Dao T. Khoa, A. Lepine-Szily, W. Mittig, W. von Oertzen, A. N. Ostrowski, P. Roussel-Chomaz, J. Siegler, M. Wilpert, Th. Wilpert, Phys. Lett. B **365**, 23 (1996).

[5] M. E. Brandan and K. W. McVoy, Phys. Rev. C **55**, 1362 (1997).

[6] M. P. Nicoli, F. Haas, R. M. Freeman, N. Aissaoui, C. Beck, A. Elanique, R. Nouicer, A. Morsad, S. Szilner, Z. Basrak, M. E. Brandan, and G. R. Satchler, Phys. Rev. **C60** 064608 (1999).

[7] Dao T. Khoa, W. von Oertzen, H. G. Bohlen and F. Nuoffer, Nucl. Phys. **A672**, 387 (2000).

[8] M. E. Brandan, A. Menchaca-Rocha, L. Trache, H. L. Clark, A. Azhari, C. A. Gagliardi, Y.-W. Lui, R. E. Tribble, R. L. Varner, J. R. Beene, G. R. Satchler, Nucl. Phys. **A668**, 695 (2001)

[9] G. Fäldt, A. Ingemarsson and J. Mahalanabis, Phys. Rev. C **46**, 1974 (1992).

[10] S. M. Eliseev and K. M. Hanna, Phys. Rev. **C56**, 554 (1997).

[11] C. E. Aguiar, F. Zardi and A. Vitturi, Phys. Rev. **C56**, 1511 (1997).

[12] T. W. Donnelly, J. Dubach and J. D. Walecka, Nucl. Phys. Nucl. Phys. **A232**, 355 (1974).

[13] D. Waxman, C. Wilkin, J. -F. Fermond and R. J. Lombard, Phys. Rev. C **24**, 578 (1981).

[14] M. H. Cha and Y. J. Kim, Phys. Rev. **C51**, 212 (1995).

[15] Y. J. Kim, M. H. Cha, Int. J. Mod. Phys. **E9**, 67 (2000).

E_{lab} = 250 MeV 에서 ^{16}O + ^{16}O 계의 굴절성 탄성산란

김용주, 현남규

제주대학교 물리학과, 기초과학연구소, 제주 690-756

강동식

제주대학교 과학교육과, 제주 690-756

요 약

E_{lab} = 250 MeV에서 ^{16}O + ^{16}O 계의 탄성산란에 대한 실험 데이타가 충돌핵 사이의 쿨롱궤적에 기초한 제 1 차 Eikonal 모형의 틀 내에서 분석되었다. 고전적 편향함수를 통하여 이 계에서 핵 무지개 현상의 존재를 확인할 수 있었다. E_{lab} = 250 MeV에서 ^{16}O + ^{16}O 계의 굴절성 탄성산란을 기술하기 위해서는 강한 실수 퍼텐셜과 약한 허수 퍼텐셜이 요구되는 것을 알 수 있었다. 굴절성 패턴은 작은 핵 반경에서 광학 실수 퍼텐셜에 매우 민감함을 보여주었다.